Romanian Reports in Physics, Vol. 67, No. 2, P. 483–493, 2015

TOTAL EXCITATION ENERGY PARTITION BETWEEN FULLY ACCELERATED FISSION FRAGMENTS IN THE FRAME OF THE POINT-BY-POINT MODEL*

I. VISAN[1, 2], G. GIUBEGA[1], A. TUDORA[1]

[1] University of Bucharest, Faculty of Physics, Bucharest-Magurele, POB MG-11, R-76900, Romania;
E-mail: iuliana.visan@yahoo.com; giubega_georgiana@yahoo.com; anabellatudora@hotmail.com
[2] Institute for Nuclear Research, POB 78, 115400-Mioveni, AG, Romania,
E-mail: iuliana.visan@nuclear.ro

Received August 12, 2013

Abstract. The systematic behaviour of the experimental ratio of the heavy fragment prompt neutron multiplicity to the multiplicity of the fragment pair allows parameterizations of the corresponding excitation energy ratio. The excitation energies of the fission fragments calculated by modeling at scission were parameterized using simple linear functions. The validation of these parameterizations was done by Point-by-Point model calculations for ^{235}U(n,f) and ^{239}Pu(n_{th},f) benefiting of experimental data of prompt neutron multiplicity as a function of fragment mass. Similar excitation energy parameterizations are performed for other fissioning systems for which experimental data are very scarce or totally missing. Using these parameterizations in the frame of Point-by-Point model, prompt emission data can be predicted for any fissioning systems.

Key words: total excitation energy, fissioning systems, prompt emission data.

1. INTRODUCTION

The present paper presents Point-by-Point (PbP) model calculations of the prompt neutron multiplicity using a new parameterization of the ratio of heavy fragment excitation energy to the total excitation energy as a function of the heavy fragment mass number (E^*_H/TXE(A_H)) [1]. This ratio can be obtained from the modeling at scission providing the fragment excitation energy at full acceleration ($E^*(A)$). The knowledge how the total excitation energy (TXE) is partitioned between the fully accelerated fission fragments (FF) is crucial in prompt emission model calculations. Nowadays, several methods of TXE partition are used in the frame of two prompt emission approaches: a deterministic one, the PbP model [2] (used in the present work) and a probabilistic Monte-Carlo (MC) treatment included in the FIFRELIN code developed at CEA Cadarache.

* Paper presented at the Annual Scientific Session of Faculty of Physics, University of Bucharest, June 21, 2013, Bucharest-Magurele, Romania.

In the frame of PbP treatment, two methods of TXE partition were developed by the fission group of the University of Bucharest as following:

– A method based on the systematic behavior of the experimental prompt neutron multiplicity data as function of fragment mass number $\nu(A)$ [3].

– A method based on modeling at scission [4]. This method was included in a newly FORTRAN 95 code used in the present work. The $E^*(A)$ results for several fissioning systems, provided by this code, put as ratio of $E^*_H/\mathrm{TXE}(A_H)$, exhibit a regular behavior that can be parameterized. The obtained parameterizations are directly used in PbP model calculations.

These parameterizations are validated by the PbP results of $\nu(A)$ describing very well the experimental data of ^{239}Pu(n_{th},f) and ^{235}U(n,f) at the incident energies of 0.5 MeV and 5.5 MeV. Similar excitation energy parameterizations resulting from the modeling at scission are performed for other fissioning systems for which experimentally prompt emission data are very scarce or totally missing, *e.g.* ^{240}Pu(SF), ^{234}U(n,f) and ^{232}Th(n,f).

2. BRIEF DESCRIPTION OF MODELS USED

The present calculations of TXE partition between the fully accelerated FF are made in the frame of Point-by-Point [2] treatment using the method based on modeling at scission [4]. Briefly, this method consists in two important steps:

1) The calculation of extra-deformation energies of nascent fragments at scission with respect to full acceleration using deformability – based on liquid drop model with shell corrections taken into account and β_2 deformation parameters provided by Hartree-Fock-Bogoliubov [5] calculations.

2) The calculation of the available excitation energy at scission which is obtained by subtracting the extra-deformation energies of nascent fragments at scission from the total excitation energy at full acceleration. The available excitation energy at scission is shared between the complementary nascent FF assuming the thermodynamic equilibrium at scission and Fermi-Gas description of the fragments level densities. The excitation energies and fragments level densities at scission are obtained concomitantly using an iterative procedure in the frame of the generalized superfluid model of Ignatyuk [6].

Finally, the fragment excitation energy at full acceleration is obtained as a sum of the extra-deformation energy (step 1) and the excitation energy at scission (step 2) for all fission fragments forming the fragmentation range of the PbP treatment.

In the Point-by-Point model calculations, the fragment excitation energy provided by different TXE partition methods *e.g.* the modeling at scission [4], different parameterizations as $\nu_H/\nu_{pair}(A_H)$ [3] or $E^*_H/\mathrm{TXE}(A_H)$ [1] are used.

The basic features of the Point-by-Point model [2] can be synthetized as following:

a. The fragmentation range plays a very important role in Point-by-Point model calculations. This is generated taking into account the entire FF mass range (for the symmetric fission up to a far asymmetric split). For each fragment mass one, two, three or four charge numbers are chosen as the nearest integer values above and below the most probable charge obtained from "unchanged charge distribution" (Z_{UCD}) corrected with a possible charge polarization (ΔZ). For each fragment pair of the fragmentation range, all quantities are calculated for total kinetic energies values (TKE) covering a convenient range.

b. The primary result of the Point-by-Point model consists in the multi-parametric matrices of all quantities characterizing both the FF and the prompt emission data (generically labeled q (Z, A, TKE)). These matrices do not depend on experimental data. To provide q (Z, A, TKE), the PbP model only needs data taken from reference parameter libraries such as mass excesses and shell corrections from RIPL3 [7] and optical model potential parameterizations needed for the calculation of compound nucleus cross-sections of the inverse process of neutron evaporation from all FF involved (also taken from RIPL3 [8]) .

c. The PbP model is able to provide almost all quantities characterizing the prompt emission: average quantities as a function of fragment mass (e.g. $< \nu >((A))$, average quantities as a function of TKE (*e.g.* $<\nu>$(TKE)) or total average ones (e.g. $< \nu_p >$, PFNS). These data are obtained by averaging the corresponding multi-parametric matrices over different fragment distributions: the charge distribution $p(Z, A)$ (usually taken as a narrow Gaussian function [9]) and the fragment mass and TKE distribution $Y(A,\mathrm{TKE})$, which are usually experimental data.

To obtain the average quantities as a function of fragment mass, the corresponding matrix is averaged over charge and total kinetic energy distributions [2, 10]:

$$< q > (A) = \sum_{Z,TKE} q(Z,A,\mathrm{TKE})\; p(Z,A)\; Y(A,\mathrm{TKE}) \Big/ \sum_{Z,TKE} p(Z,A)\; Y(A,\mathrm{TKE}). \qquad (1)$$

Average quantities as a function of TKE are obtained by averaging the corresponding matrix over charge and mass distributions:

$$< q > (\mathrm{TKE}) = \sum_{Z,A} q(Z,A,\mathrm{TKE})\; p(Z,A)\; Y(A,\mathrm{TKE}) \Big/ \sum_{Z,A} p(Z,A)\; Y(A,\mathrm{TKE}) \qquad (2)$$

The total average quantities are obtained by averaging the corresponding matrix over charge, mass and TKE distributions:

$$< q >= \sum_{Z,A,TKE} q(Z,A,\mathrm{TKE})\; p(Z,A)\; Y(A,\mathrm{TKE}) \Big/ \sum_{Z,A,TKE} p(Z,A)\; Y(A,\mathrm{TKE}). \qquad (3)$$

The mass and TKE distributions of the fission fragments needed in present calculations were measured at Institute for Reference Materials and Measurements, Geel, Belgium (IRMM) in the case of ^{234,235}U(n,f) [11] or were taken from EXFOR[12] for ^{239}Pu(n_{th},f), ^{240}Pu(SF) and ^{232}Th(n,f).

3. RESULTS AND DISCUSSIONS

For all fissioning systems for which experimental ν(A) data exists, it was observed that the ratio $\nu_H/\nu_{pair}(A_H)$ exhibits a systematic behaviour that is similar with the behaviour of the ratio E^*_H/TXE(A_H) obtained from the modeling at scission [13]. This representation, focused on the heavy fragment group allowing to observe systematic behaviours, was preferred in the place of the traditional ν(A) or $E^*(A)$, because the nuclei forming the heavy fragment group are not changing significantly from one fissioning system to another.

The $E^*(A)$ results obtained by modeling at scission reveal the same systematic behaviour of the ratio E^*_H/TXE(A_H) as the experimental ratio $\nu_H/\nu_{pair}(A_H)$ [13] consisting in: ν_H/ν_{pair} is less than 0.5 for fragments pairs with $A_H < 140$, with a minimum around $A_H = 130 \div 132$ (driven by the magic numbers $Z = 50$ and $N = 82$); ν_H/ν_{pair} is approximately 0.5 for fragmentations with A_H around 140 and it exhibits an almost linear increase for A_H above 140.

An example of E^*_H/TXE (A_H) is presented in Fig.1 [1], for ^{235}U(n, f) in the upper part and for ^{239}Pu(n_{th},f) in the lower part. The results of modeling at scission are plotted with full blue circles in comparison with the "indirect experimental data" (plotted with different open symbols). The linear parameterizations are plotted with red solid lines.

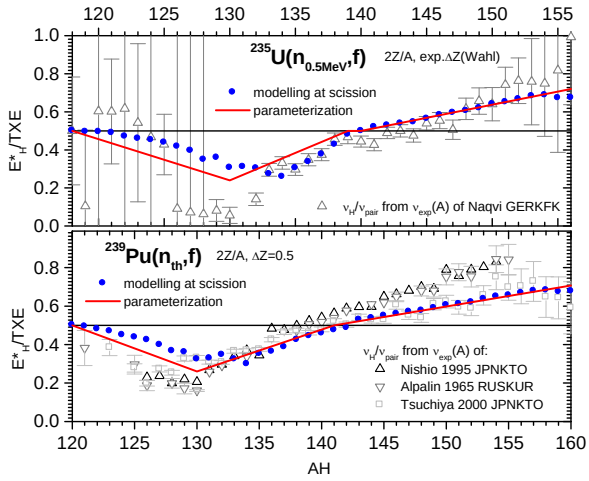

Fig. 1 – E^*_H/TXE parameterization in comparison with the results of modeling at scission and the experimental data for ^{235}U ($n_{0.5MeV}$,f) (upper part) and for ^{239}Pu(n_{th},f) (lower part).

Examples for the validation of the E^*_H/TXE parameterization are given in Figs. 2, 3 for ^{235}U(n,f) and ^{239}Pu(n_{th},f), respectively. In both figures, the $E^*(A)$ resulted from modeling at scission (plotted with red circles at E_n = 0.5 MeV and blue diamonds at E_n = 5.5 MeV in Fig. 2 and with blue circles in Fig. 3) and from

the linear parameterization (small symbols connected with lines only to guide the eye) are very close each to other and describe very well the "indirect E^* experimental data" [4].

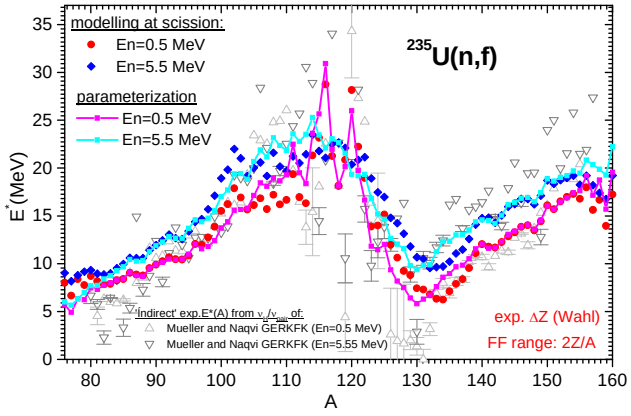

Fig. 2 – ^{235}U(n,f): $E^*(A)$ resulted from the modeling at scission and from the parameterization in comparison with the "indirect experimental data".

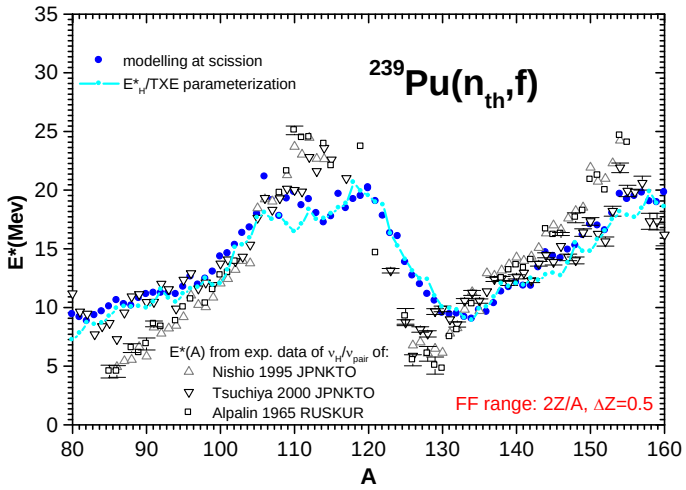

Fig. 3 – ^{239}Pu(n_{th},f): $E^*(A)$ resulted from the modeling at scission and from the parameterization in comparison with the "indirect experimental data".

In Fig. 4, the PbP calculations of $\nu(A)$ for ^{235}U(n,f) using the E^*_H/TXE parameterization given in the upper part of Fig.1 (plotted with red squares at $E_n = 0.5$ MeV and blue diamonds at $E_n = 5.5$ MeV) describe very well the experimental data [14] (different grey symbols) including the interesting behaviour of multiplicity increasing with E_n for heavy fragments mainly.

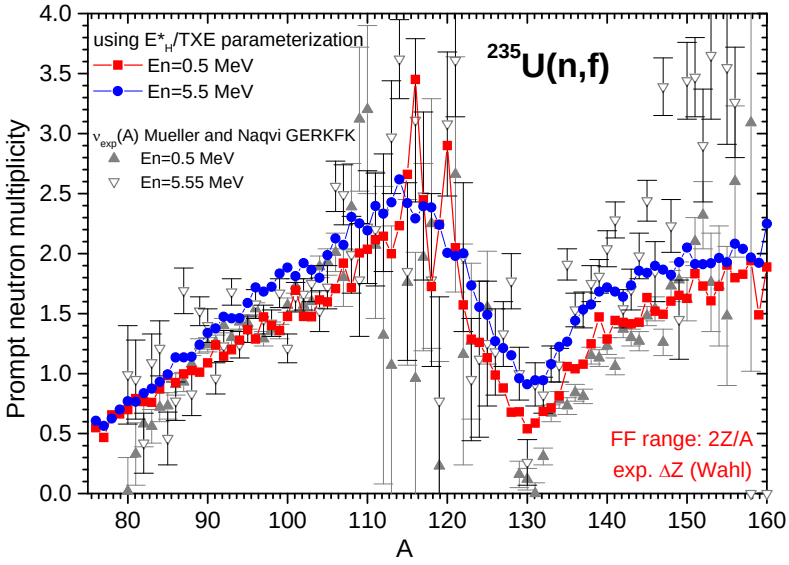

Fig. 4 – ^{235}U(n,f): PbP results of ν(*A*) obtained by using the *E**$_{H}$/TXE parameterization.

In the case of ^{239}Pu(n$_{th}$,f), the ν(*A*) results (given in Fig. 5 with green circles) obtained by using the present *E**$_{H}$/TXE parameterization (given in the lower part of the Fig.1) are in good agreement with the experimental data [15].

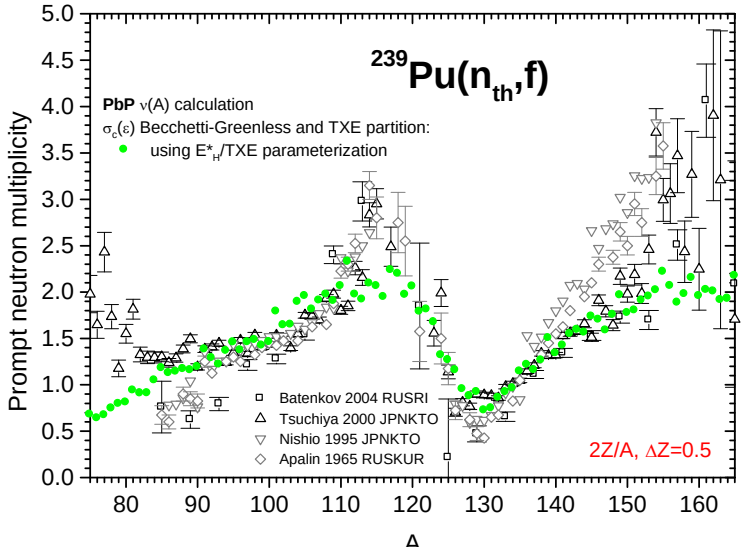

Fig. 5 – ^{239}Pu(n$_{th}$,f): PbP results of ν(*A*) obtained by using the *E**$_{H}$/TXE parameterization.

Similar calculations were performed for both induced and spontaneous fissioning systems with scarce or totally missing experimental data, as following:

– ^{234}U(n,f) at 14 incident energies values ranging from 0.2 MeV to 5 MeV (benefiting of recently fragment distributions measured at IRMM [11])

– ^{232}Th(n,f) at 6 incident energies ranging from 1.6 MeV to 5.8 MeV for which fragment distributions exist in EXFOR [12])

– ^{240}Pu(SF) using the fragment distributions also taken from EXFOR [12].

For all cases mentioned above, linear parameterizations of E^*_H/TXE (A_H) were performed. A few examples of $E^*(A)$ results obtained by modeling at scission and using the obtained parameterizations are plotted in Figs. 6, 7, 8.

In Fig. 6 and Fig. 7, the $E^*(A)$ and $\nu(A)$ results for ^{234}U(n,f) and ^{232}Th(n_{th},f) respectively, are given at several incident energies. As can be seen in these figures, the results of $E^*(A)$ obtained from the linear parameterizations are very close to those from modeling at scission. Both for ^{234}U(n,f) and ^{232}Th(n,f), the PbP results of $\nu(A)$ obtained using the present parameterization exhibit the interesting behavior consisting in the ν-increase with E_n for heavy fragments mainly.

The case of ^{240}Pu fissioning system from the ground state (^{240}Pu(SF)) and from the excitation energy ($E^* = B_n = 6.5335$ MeV) (^{239}Pu(n_{th},f)) is given in Fig.8. The $E^*(A)$ behaviour (that is practically the same with the $\nu(A)$ behaviour) does not confirm the increase with E_n for heavy fragments mainly. Both calculations, modeling at scission (red and blue symbols) and present parameterizations (magenta and cyan symbols connected with lines), are again close each to other.

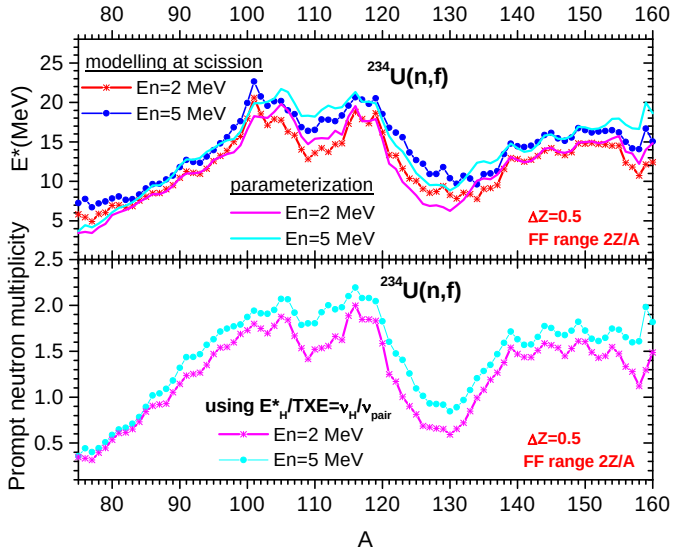

Fig. 6 – ^{234}U(n,f):$E^*(A)$ resulted from the E^*_H/TXE parameterization (upper part), PbP results of $\nu(A)$ (lower part) calculated by using $E^*(A)$ plotted in the upper part.

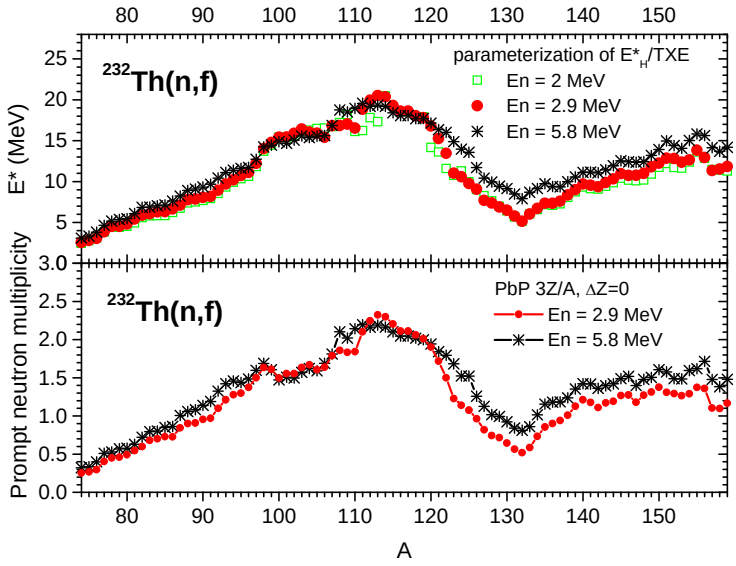

Fig. 7 – ^{232}Th(n,f):$E^*(A)$ resulted from the E^*_H/TXE parameterization (upper part), PbP results of $\nu(A)$ (lower part) calculated by using $E^*(A)$ plotted in the upper part.

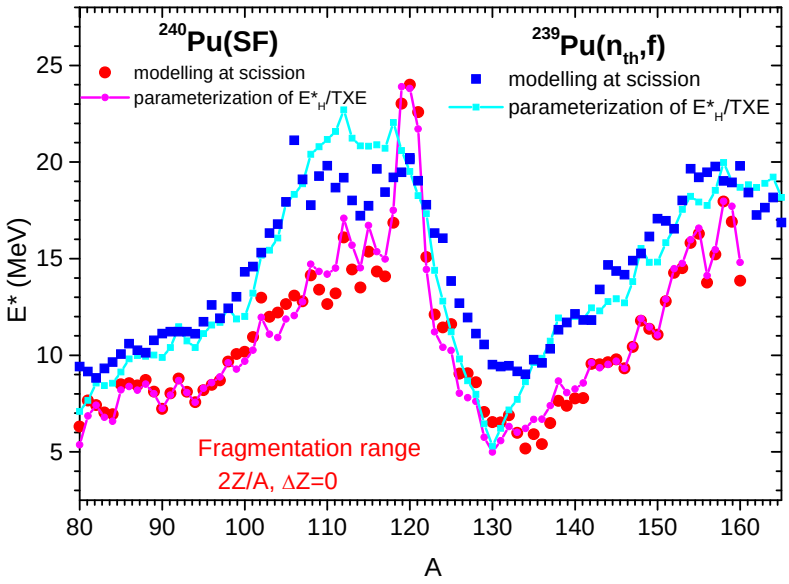

Fig. 8 – Comparison between $E^*(A)$ resulted from modeling at scission and $E^*(A)$ from the E^*_H/TXE parameterization for ^{240}Pu(SF) and ^{239}Pu(n_{th},f).

An interesting finding that deserves to be mentioned is the insensibility of the fragment pair multiplicity ($\nu_{pair} = \nu_L+\nu_H$) to the TXE partition. This fact is proved by very close ν_{pair} (A_H) results obtained by very different TXE partitions used in the same model and by different models using different TXE partitions as following:

– Point-by-Point model using $E^*(A)$ from modeling at scission, from parameterizations or even the very rough TXE partition ($E^*_H = E^*_L$ = TXE/2)

– Very different approaches: the present deterministic PbP model and the probabilistic Monte Carlo treatment [13, 16] (FIFRELIN code of CEA Cadarache) using different TXE partitions.

An example is given for the case of ^{239}Pu(n_{th},f) for which $\nu_{pair}(A_H)$ resulted from different ν(A) model calculations using different TXE partitions are plotted in Fig. 9 together with the experimental data taken from EXFOR [15]. As can be seen all ν_{pair} results are close to each other and also in good agreement with experimental data. Even the very rough approximation of TXE/2 gives ν_{pair} results very close to all other ones.

This fact is exemplified in Fig. 9 for ^{239}Pu(n_{th},f). $\nu_{pair}(A_H)$ provided by PbP calculations using the present parameterization (magenta circles) and using the rough TXE/2 partition (open wine circles) are practically identical. The Monte Carlo results obtained with two different TXE partition driven by different RT functions (blue and cyan diamonds) are also almost identical. Moreover, the PbP and the FIFRELIN results are close each to others, too, and in good agreement with the experimental data (different grey open symbols).

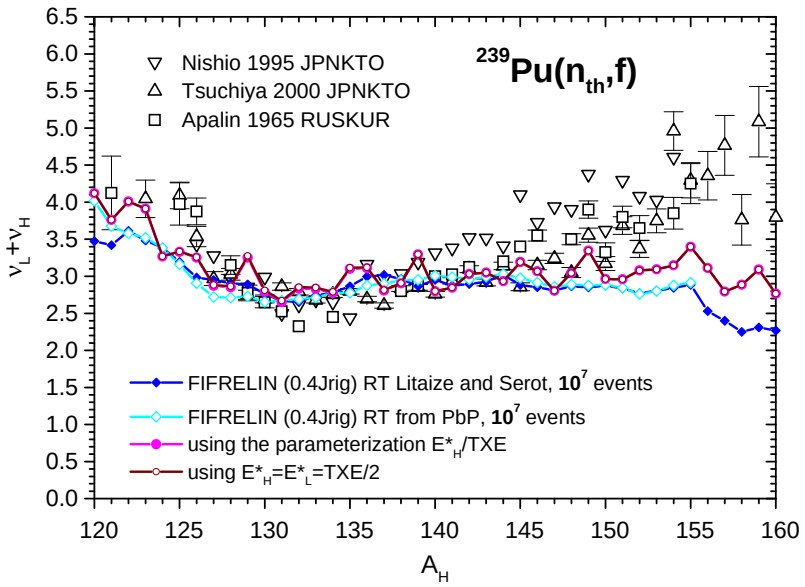

Fig. 9 – ^{239}Pu(n_{th}, f): ν_{pair} results from E^*_H/TXE parameterization in comparison with different results obtained with different TXE partitions.

4. CONCLUSIONS

1. The partition of the total excitation energy between fully accelerated fission fragments obtained from the modeling at scission revealed a systematic behaviour of the ratio E^*_H/TXE(A_H) that is similar with the behaviour of experimental ν_H/ν_{pair} (A_H) ratio.

2. This systematic behaviour of E^*_H/TXE(A_H) allows simple linear parameterizations that can be used in the PbP model (instead of the fragment excitation energy resulted from the modeling at scission) to provide/ predict prompt emission data in a shorter computing time.

3. The inter-comparison of the obtained results for the studied fission systems as well as their comparison with the existing experimental data revealed some interesting facts which can be synthesized as following:

– An increasing of $E^*(A)$ with the incident energy, reflected in an increasing of $\nu(A)$ for heavy fragments only is obtained for all studied neutron induced fissioning systems, confirming the experimental observations and the results of other models.

– The insensibility of the fragment pair multiplicity to the TXE partition is verified by the PbP model calculations using many and very different TXE partitions and also by the comparison with ν_{pair} results of the Monte Carlo treatment.

Acknowledgements. One of the authors (I.V.) is very grateful to Andrei Rizoiu from Institute for Nuclear Research Pitesti for suggestions and valuable help of FORTRAN programming given during this work.

REFERENCES

1. I. Visan, G. Giubega, A. Tudora, *The 6th Annual International. Conference on Sustainable Development through Nuclear Research and Education*, Proceeding ISSN-20-66-2955, Piteşti, România, May 22–24, 2013.
2. A. Tudora, Ann. Nucl. Energy, **53**, 507–518 (2013).
3. C. Manailescu, A. Tudora, F.-J. Hambsch, C. Morariu, S. Oberstedt, *Possible reference method of total excitation energy partiţion between complementary fission fragments*, Nucl. Phys., **A 867**, 12–40 (2011).
4. C. Morariu, A. Tudora, F.-J. Hambsch, S. Oberstedt, C. Manailescu, *Modelling of the total excitation energy partiţion including fragment deformation and excitation energies at scission*, J. Phys., **G 39**, 055103 (2012).
5. *Reference Input Parameter Library of IAEA* (RIPL–3), Segment 1 *Deformations*, database HFB-14, 2012 c; S. Goriely, M. Samyn and J. M. Pearson, Phys. Rev., **C 75**, 064213 (2007).
6. A. Ignatyuk, IAEA-RIPL1, *IAEA TECDOC*-1034, Segment V (Chapter 5.1.4), 1998.
7. Reference Input Parameter Library of IAEA, (RIPL–3), Segment 1 *Nuclear Masses and Deformations* database of Audi and Wapstra (mass excesses) and of Moller and Nix (shell corrections) (2012b), available online http://www-nds.iaea.org,.
8. *Reference Input Parameter Library of IAEA*, (RIPL-3), Electronic file from segment *Optical Model Parameters*', ID 100 Becchetti-Greenless, (2011a) http://www-nds.iaea.org.
9. C. Wagemans, *The Nuclear Fission Process*, CRC Press, Boca Raton, USA, 1991.

10. I. Visan, A. Tudora, C. Manailescu, *Experimental average prompt neutron multiplicity as a function of total kinetic energy of fission fragments described by Point-by-Point model calculations*, Int. Nucl. Data Conf., NY, USA, 2013.
11. Al-Adili, A., Hambsch, F. J., Pomp, S., Obserstedt, S., Internat. Workshop *GAMMA-1*, Novi Sad, Serbia, November 2011; Physics Procedia, **31**, 158–164 (2012).
12. Experimental Nuclear Reaction Data Base, EXFOR Targets Th-232, Pu-239, Pu-240, reactions (n,f) and (0,f), quantities AKE FF 2013.
13. C. Manailescu, Ch. IV, PhD Thesis, University of Bucharest, 2013.
14. Experimental Nuclear Reaction Data Base, EXFOR target, 235U, Reaction (n,f), Quantity MFQ, available online http://www-nds.iaea.org/EXFOR 2011.
15. Experimental Nuclear Reaction Data Base, EXFOR Target Pu-239, Reaction (n,f), Quantity MFQ, Data of Nishio *et al*. (entry 23012), Tsuchiya *et al*. (entry 22650), Apalin (entry 41397).
16. Litaize, O., Serot, O., Phys. Rev. C, **82**, 054616 (2010).